Hydrodynamic Consideration on Added Resistance and Ship-generated Unsteady Waves

Masashi Kashiwagi, Takuma Sasakawa and Tomoki Wakabayashi

Department of Naval Architecture & Ocean Engineering, Osaka University
2-1 Yamada-oka, Suita, Osaka 565-0871, Japan E-mail: *kashi@naoe.eng.osaka-u.ac.jp*

Abstract

In order to investigate which component or part of ship-generated unsteady waves is dominant in the added resistance, measurements of unsteady waves and the subsequent unsteady wave analysis using the Fourier transform to compute the added resistance are carried out for canonical problems of the wave diffraction, the forced oscillations in heave and pitch, and the free-response of ship motions in head waves. With these results, validity of the linear superposition of component waves is studied and discussion is made on associated nonlinear effects in the wave generation and dominant wave components in the added resistance.

1. Introduction

When a ship advances in waves, the resistance on the ship increases as compared to that in calm sea. This increase of resistance is called the added resistance. Since Maruo's pioneering work, it has been well recognized that the dominant component in the added resistance is the one due to generation of unsteady waves and their interaction with incident wave. Notwithstanding a large amount of work so far, details of the hydrodynamic relation between the added resistance and ship-generated unsteady waves seem to be unclear, because most comparisons have been made between the total increase in the ship resistance measured by a dynamometer in waves and the calculated value with a simplified potential-flow theory. In order to evaluate accurately the amount of unsteady wave-making resistance and to understand hydrodynamic relations with ship disturbance waves (for instance, which component or which part of unsteady waves is dominant in the added resistance), it is useful to apply the unsteady wave-pattern analysis proposed by Ohkusu (1980).

From that viewpoint, Kashiwagi (2010) showed in the 25th Workshop some measured results of unsteady waves using a modified Wigley model and corresponding computed results by Enhanced Unified Theory (EUT) developed by Kashiwagi (1995). In that comparison, a large discrepancy was observed near the peak of the added resistance where wave-induced ship motions also become large. Another prominent discrepancy observed in a comparison of the wave profile was that short-wavelength components in measured waves were very small in amplitude as opposed to numerical results by EUT. In order to study possible reasons of these discrepancies, additional experiments using the same modified Wigley model were newly conducted, measuring the unsteady waves for three canonical cases of the diffraction problem, the forced oscillation problem in heave and pitch, and the motion-free problem in incident waves, by means of larger number of wave probes. With these measured results together with analytical and numerical studies, discussions are made on the validity of linear superposition of the diffraction and radiation waves, and on which component in the unsteady waves is dominant in predicting the added resistance.

2. Added Resistance and Unsteady Waves

We consider a ship advancing at constant forward speed U into a regular incident wave of amplitude A, circular frequency ω_0. The depth of water is assumed infinite; thus the wavenumber of incident wave is given by $k_0 = \omega_0^2/g$, with g the acceleration due to gravity. Corresponding to the experiment, only the head wave is considered, and the analysis is made with a right-hand Cartesian coordinate system O-xyz, with the origin placed at the center of a ship and on the undisturbed free surface, which translates with the same constant speed as that of a ship along the positive x-axis. The z-axis is positive downward. Unsteady ship responses and ambient unsteady flow of fluid are assumed to be linear and periodical with circular frequency of encounter $\omega = \omega_0 + k_0 U$.

The added resistance in regular waves can be computed in terms of the Kochin function which can be associated with the Fourier transform of ship-generated unsteady waves. Using the Fourier transform with respect to x, as shown by Kashiwagi (2010), the calculation formula for the added resistance in head waves can be written as follows:

$$R_{AW} = \frac{\rho g}{4\pi}\left[-\int_{-\infty}^{k_1} + \int_{k_2}^{k_3} + \int_{k_4}^{\infty} \right] \left| \zeta^*(k,y) \right|^2 \times \frac{\sqrt{\kappa^2 - k^2}}{\kappa^2} \left(k + k_0 \right) dk \qquad (1)$$

where

$$\left.\begin{aligned} \kappa &= \frac{1}{g}\left(\omega + kU\right)^2 = K + 2k\tau + \frac{k^2}{K_0} \\ K &= \frac{\omega^2}{g},\ \tau = \frac{U\omega}{g},\ K_0 = \frac{g}{U^2} \end{aligned}\right\} \qquad (2)$$

$$\left.\begin{matrix} k_1 \\ k_2 \end{matrix}\right\} = -\frac{K_0}{2}\left(1 + 2\tau \pm \sqrt{1+4\tau}\right) \qquad (3)$$

$$\left.\begin{matrix} k_3 \\ k_4 \end{matrix}\right\} = \frac{K_0}{2}\left(1 - 2\tau \mp \sqrt{1-4\tau}\right) \qquad (4)$$

For $\tau > 1/4$, k_3 and k_4 become complex and the integration range in (1) must be treated as continuous for $k_2 < k$. $\zeta^*(k,y)$ in (1) is the Fourier transform defined as

$$\zeta^*(k,y) = \int_{-\infty}^{\infty} \zeta(x,y)\, e^{ikx}\, dx \qquad (5)$$

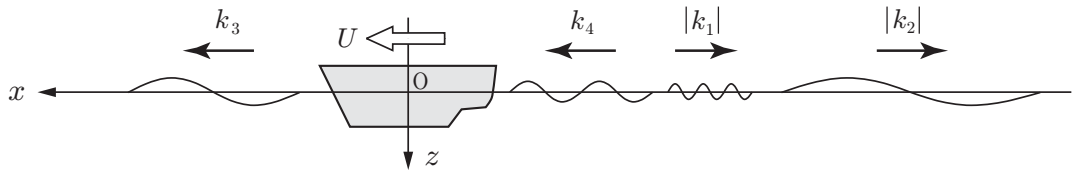

Fig. 1 Coordinate system and schematic illustration of wave components

where $\zeta(x,y)$ denotes the ship-generated unsteady wave, which is assumed in the linear theory to be given by the linear superposition of scattering wave $\zeta_7(x,y)$ and radiation waves $\zeta_j(x,y)$ by surge ($j=1$), heave ($j=3$) and pitch ($j=5$) motions, as in the following form:

$$\zeta(x,y) = A\,\zeta_7(x,y) + \sum_{j=1,3,5} X_j\,\epsilon_j\,\zeta_j(x,y) \tag{6}$$

where X_j is the complex amplitude in the j-th mode of motion and symbol ϵ_j is adopted to express the length dimension for pitch; that is, $\epsilon_5 = L/2$ and $\epsilon_j = 1$ for surge and heave.

Here in head waves $\omega = \omega_0 + k_0 U$, which gives

$$\left.\begin{aligned} \omega_0 &= \frac{g}{2U}\big(-1+\sqrt{1+4\tau}\big) > 0 \\ k_0 &= \frac{\omega_0^2}{g} = \frac{K_0}{2}\big(1+2\tau-\sqrt{1+4\tau}\big) = -k_2 = |k_2| \end{aligned}\right\} \tag{7}$$

On the other hand, we can prove that the relations between the ship's speed U and the phase velocity c of component wave k_j ($j=1,3,4$) are

$$\left.\begin{aligned} 0 < U < \frac{c}{2} \quad & \text{for } k_3\text{-wave} \\ \frac{c}{2} < U < c \quad & \text{for } k_4\text{-wave} \\ c < U \quad & \text{for } k_1\text{-wave} \end{aligned}\right\} \tag{8}$$

Since $c/2$ is equal to the group velocity with which the wave energy is transported, we can understand the location of existence, the relative wavelength, and the travelling direction when viewed from a ship moving at forward speed U, for each of the component waves k_j ($j=1\sim4$); these are schematically shown in Fig. 1. We note that at $\tau = 1/4$, $k_3 = k_4$ and U becomes equal to the group velocity of wave.

3. Dominant Components in Added Resistance

In reality, the wavenumber of progressive waves generated by a ship varies over the integration range shown in (1). In order to see which component of progressive waves contributes predominantly to the added resistance, we will check the values of the integrand of (1), by rewriting (1) in the form

$$R_{AW} = \frac{\rho g}{4\pi}\left[-\int_{-\infty}^{k_1} + \int_{k_2}^{k_3} + \int_{k_4}^{\infty}\right] W_1(k)\,W_2(k)\,dk \tag{9}$$

where

$$W_1(k) = \big|\,\zeta^*(k,y)\big|^2 \tag{10}$$

$$W_2(k) = \frac{\sqrt{\kappa^2-k^2}}{\kappa^2}\big(k+k_0\big) \tag{11}$$

Here it should be noted that $W_2 = 0$ at $k = k_j$ ($j=1\sim4$) because of $\kappa^2 = k^2$, and $k + k_0 = k - k_2$ by (7). When computing the added resistance for the case of forced oscillation problem (i.e. the radiation problem), $k + k_0$ in (11) must be replaced simply with k, because the term related to k_0 in (11) represents interactions between the incident wave and ship-disturbance wave. Numerical examples of $W_1(k)$ and $W_2(k)$ will be shown in the Workshop due to paucity of enough space in this paper.

In order to understand qualitatively the dominant wave components and general characteristics in the Fourier transform of the wave, let us consider a wave component, propagating in the positive x-axis with wavenumber k_ℓ and amplitude of the following form:

$$\zeta(x,y) = \alpha\,\frac{u(x_s-x)}{\sqrt{|x-x_s|}}\,e^{-ik_\ell x} \tag{12}$$

where α denotes the amplitude coefficient, x_s the starting point of wave existence along a line parallel to the x-axis, and $u(x_s-x)$ the unit step function.

The Fourier transform of this wave may be expressed as

$$\begin{aligned} \zeta^*(k,y) &= \int_{-\infty}^{\infty} \zeta(x,y)\,e^{ikx}\,dx \\ &= \alpha\sqrt{\frac{\pi}{|k-k_\ell|}}\,e^{i(k-k_\ell)x_s}\,e^{i\frac{\pi}{4}\mathrm{sgn}(k-k_\ell)} \end{aligned} \tag{13}$$

Therefore it is obvious that the value of $W_1(k)$ becomes large at $k = k_\ell$ and decays in proportion to $1/|k-k_\ell|$.

For larger values of k, $W_2(k)$ becomes small at order of $O(1/k)$ and the amplitude coefficient α must be small in reality for waves with large k (small wavelength). As already noted, k_j ($j=1\sim4$) is a root of $\kappa^2 - k^2 = 0$, and $k + k_0 = k - k_2$. Hence, dominant wave components in the added resistance may be relatively longer waves with smaller value of k satisfying $k_2 < k$. We note that if $k_2 < k < 0$, the wave propagates in the negative x-axis like k_2-wave in Fig. 1, and if $0 < k$, the wave propagates in the positive x-axis like k_3- and k_4-waves in Fig. 1.

4. Experiments

In order to see the degree of contribution of each wave $\zeta_j(x,y)$ expressed in Eq. (6) to the added resistance, the experiments were conducted for the cases of wave diffraction (where ship motions are completely fixed), forced oscillation in heave and pitch (where incident waves are absent), and free-response of ship motions in head waves (where surge, heave, and pitch are free to respond to waves). Measured in these experiments are principally the added resistance by a dynamometer and ship-generated unsteady waves using a larger number of wave probes, and also ship motions in the motion-free case.

In the unsteady wave analysis, the number of wave probes was increased up to 12 from 6 used in the experiment last year to confirm the resolution accuracy particularly for short-wavelength waves. Those wave probes were positioned with almost equal intervals over the distance of ship's movement in one period of encounter along a longitudinal line parallel to the x-axis (at constant y). Using the least-square method in terms of the data measured with 12 wave probes,

the x-direction distribution was obtained of cosine and sine coefficients in the Fourier-series expansion for the unsteady wave oscillating at circular frequency of encounter.

The ship model used in the experiments is the same as that used in the previous experiment; that is, a modified Wigley model expressed mathematically as

$$\left.\begin{aligned}\eta &= (1-\zeta^2)(1-\xi^2)(1+0.6\xi^2+\xi^4)\\ &\quad +\zeta^2(1-\zeta^8)(1-\xi^2)^4\\ \xi &= x\frac{2}{L},\quad \zeta = y\frac{2}{B},\quad \zeta = \frac{z}{d}\end{aligned}\right\} \tag{14}$$

where the real dimensions are $L = 2.5$ m, $B = 0.5$ m, $d = 0.175$ m. The gyrational radius in pitch and the center of gravity were set equal to $\kappa_{yy}/L = 0.238$ and $\overline{OG}/d = 0.189$ (below the free surface).

The lateral distance of a longitudinal line used for the wave measurement from the centerline of a ship (x-axis) was set equal to $y = B/2+$ 0.1 m = 0.35 m. The Froude number was $Fn = 0.2$ in all measurements.

5. Results and Discussion

Figures 2 through 5 show comparisons of the added resistance for the cases of wave diffraction (Fig. 2), forced heave (Fig. 3), forced pitch (Fig. 4), and free-response of ship motions in waves (Fig. 5). Basically the results measured directly by a dynamometer are shown by closed circles, the results obtained from the unsteady wave analysis are shown by open circles, and computed results by Enhanced Unified Theory (EUT) are shown by the solid line or other symbols. It is confirmed in numerical computations by EUT that the added resistances computed directly from the Kochin function and from the wave-pattern analysis method using computed wave profile are virtually the same.

In Fig. 2, we can observe that the results by the unsteady wave analysis are in good agreement with computed ones by EUT, but those are almost half of the value by the direct measurement irrespective of the wavelength tested. This implies that nonlinear local wave generation, including wave breaking, may exist in the wave diffraction problem.

In the forced-oscillation problem shown as Figs. 3 and 4, the agreement between EUT and the results of unsteady wave analysis is generally favorable, and noticeable discrepancy from the results by the direct measurement can be observed in the short-wavelength range especially in forced pitch oscillation. This discrepancy may be attributed to nonlinear local wave generation which cannot be explained by a linear potential-flow theory. However in this short-wavelength range, actual amplitudes of ship motions are normally very small. Thus little effects will arise from this discrepancy on the total value of the added resistance.

Measured results shown in Fig. 5 for the motion-free case are essentially the same as those obtained in the experiment one year ago. A large discrepancy can be seen between the results by the direct measurement and the wave analysis using measured waves, particularly near the peak around $\lambda/L = 1.1$. In order to investigate a possible reason for this discrepancy, the wave profile was computed by the linear superposition according to Eq. (6), using the component waves obtained by the experiments of wave diffraction ($j = 7$), forced heave ($j = 3$), and forced pitch ($j = 5$), together with complex amplitudes of heave and pitch motions measured in the motion-free experiment. (The surge mode is ignored, because the forced oscillation test in surge was not conducted.) Then the superimposed wave profile was Fourier-transformed and the added resistance was computed from Eq. (1). The results of added resistance obtained from this linear superposition of component waves and complex motion amplitudes are also shown in Fig. 5. It is remarkable that these results become much closer to the results by the direct measurement and computed by EUT, especially near the peak where ship motions also become large.

Figure 6 provides the information on the profiles of scattering and radiation waves and on the difference between the wave profiles measured by the motion-free experiment and obtained by the superposition without surge motion, for a case of $\lambda/L = 1.1$ (which corresponds approximately to $KL = 12.5$ at $Fn = 0.2$).

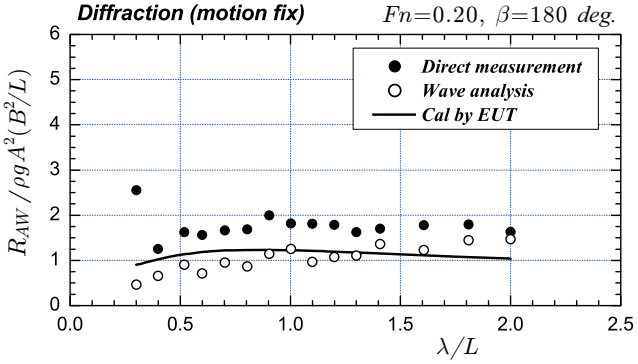

Fig. 2 Added resistance in the diffraction problem on modified Wigley model at $Fn = 0.2$

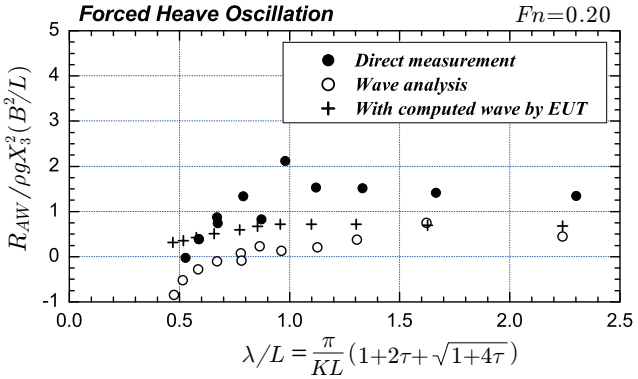

Fig. 3 Added resistance in forced heave oscillation ($X_3 =$ 0.01 m) on modified Wigley model at $Fn = 0.2$

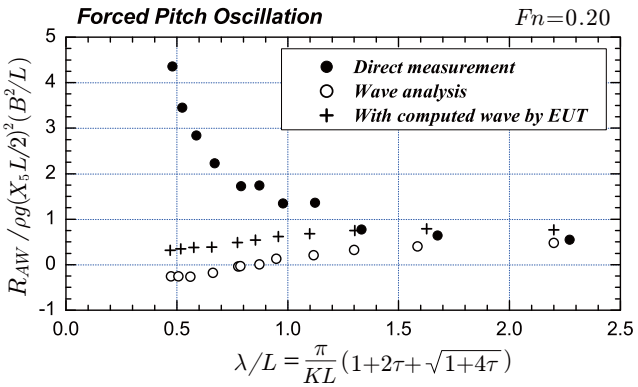

Fig. 4 Added resistance in forced pitch oscillation ($X_5 =$ 1.4 deg) on modified Wigley model at $Fn = 0.2$

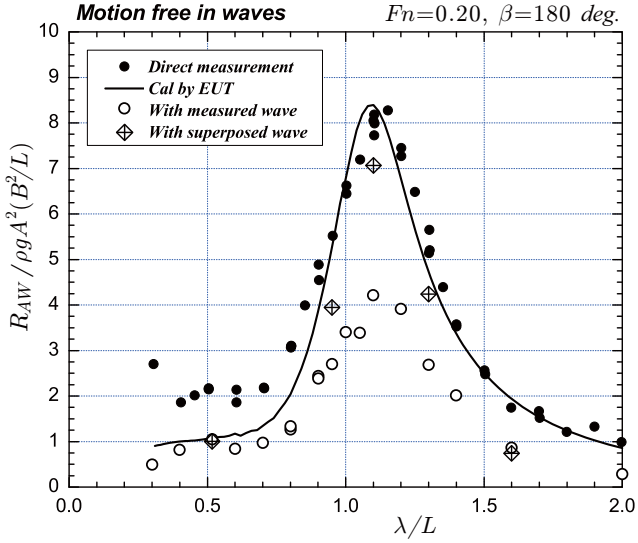

Fig. 5 Added resistance in waves (motion free) on modified Wigley model at $Fn = 0.2$

From these figures, we can see that the overall appearance of wave profile is very similar between superimposed and directly measured waves, but a large difference exists near the fore-front part of the wave. The source of this difference seems to come from the wave by the forced pitch oscillation. It is noteworthy that the forced oscillation tests were performed with relatively small amplitude ($X_3 = 0.01$ m and $X_5 = 1.4$ deg.) within the range of linear theory being valid. Therefore, when the amplitude of ship motions becomes large, linearity in the amplitude of generated wave may be violated particularly near the ship's bow due to large pitch motion, and as a result, some nonlinear local waves with energy dissipation may be generated.

6. Conclusions

By using the unsteady waves measured in the diffraction and radiation (heave and pitch only) problems and the complex amplitude of wave-induced motions, the unsteady wave corresponding to the one in the motion-free condition was produced by the linear superposition. The overall agreement in the wave was favorable, but a prominent difference was observed in the fore-front part of the wave, especially when the ship motions are large. The added resistance computed from this superimposed wave was in better agreement with the directly measured value. We can envisage from these results that, when ship motions become large, some nonlinear local waves may be generated, resulting in a noticeable discrepancy in the added resistance between the results of direct measurement and wave analysis.

References

[1] Ohkusu, M (1980). "Added Resistance in Waves in the Light of Unsteady Wave Pattern Analysis", *Proc of 13th Symp on Naval Hydrodynamics*, Tokyo, pp. 413–425.

[2] Kashiwagi, M (1995). "Prediction of Surge and Its Effect on Added Resistance by Means of the Enhanced Unified Theory", *Trans West-Japan Society of Naval Architects*, No. 89, pp. 77–89.

[3] Kashiwagi, M (2010). "Prediction of Added Resistance by Means of Unsteady Wave-Pattern Analysis", *Proc of 25th Int Workshop on Water Waves & Floating Bodies*, Harbin, pp. 69–72.

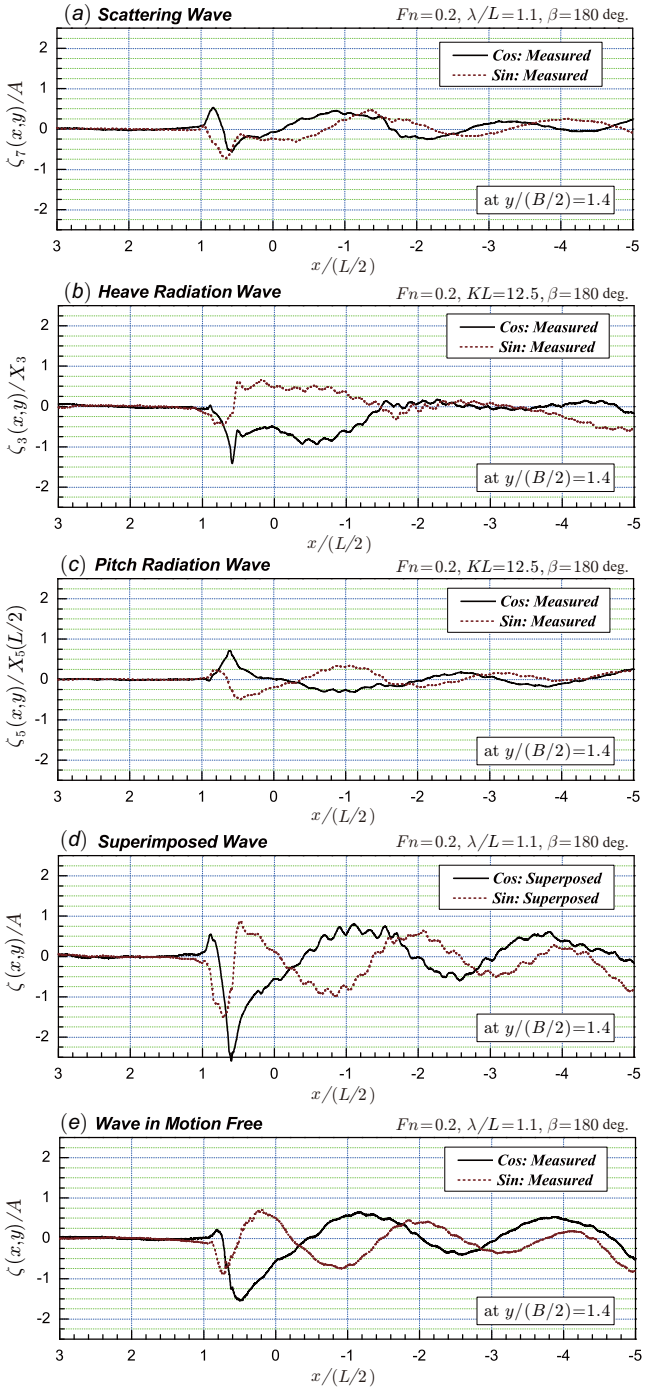

Fig. 6 Wave profiles generated by modified Wigley model at $Fn = 0.2$. (a): Scattering wave in the diffraction problem at $\lambda/L = 1.1$, (b): Radiation wave by forced heave oscillation at $KL = 12.5$ and $X_3 = 0.01$ m, (c): Radiation wave by forced pitch oscillation at $KL = 12.5$ and $X_5 = 1.4$ deg, (d): Superimposed wave using the waves of (a)∼(c) and measured complex amplitudes of heave and pitch at $\lambda/L = 1.1$, (e): Measured wave in the motion-free condition at $\lambda/L = 1.1$.